PHYSICAL REVIEW B **88**, 180404(R) (2013)

p-orbital nanomagnetism in an organic chain magnet

Wei Wu,[1,*] N. M. Harrison,[2,3] and A. J. Fisher[4]

[1]*Department of Materials and London Centre for Nanotechnology, Imperial College London, South Kensington Campus, London SW7 2AZ, United Kingdom*

[2]*Department of Chemistry and London Centre for Nanotechnology, Imperial College London, South Kensington Campus, London SW7 2AZ, United Kingdom*

[3]*Science and Technology Facilities Council Daresbury Laboratory, Daresbury, Warrington WA4 4AD, United Kingdom*

[4]*UCL Department of Physics and Astronomy and London Centre for Nanotechnology, University College London, Gower Street, London WC1E 6BT, United Kingdom*

(Received 12 August 2013; published 26 November 2013)

A long-standing challenge in spintronics is the development of a stable, processable and tunable organic magnetic semiconductor. We reveal, through first-principles calculations, that a *p*-electron organic molecular magnet, lithium phthalocyanine (LiPc), can display surprisingly strong antiferromagnetic coupling. The strong coupling, far exceeding that observed in the widely studied transition-metal phthalocyanines, is found to be due to the delocalized spin orbital of the ligand which facilitates intermolecular interactions. The enhanced hopping between the π-conjugated orbitals is also responsible for the wide bandwidth required for high spin mobility. The interactions are a strong function of the intermolecular arrangement and increase when approaching a face-on geometry resulting in a crossover to an itinerant spin density wave ground state, which we propose as an explanation for the unusual spin susceptibility in the related *x*-LiPc phase [M. Brinkmann *et al.*, J. Mater. Chem. **8**, 675 (1998)]. This strong coupling, in conjunction with the structural flexibility of the metal phthalocyanine organic semiconductors, suggests a promising route for the fabrication of transition-metal-free, room-temperature, chain magnets for spintronic applications.

DOI: 10.1103/PhysRevB.88.180404 PACS number(s): 71.70.Gm, 71.15.Mb, 71.20.Rv, 75.30.Fv

Introduction. Magnetic organic semiconductors[1–5] are promising candidates for novel spintronic devices[5–10] because they are easier to process than some conventional inorganic materials, they have long spin-lattice relaxation times (up to seconds), and there is scope for wide structural variation using the techniques of organic synthesis. The intermolecular exchange interactions determine the magnetic ordering temperature (if any) and are important parameters for spintronics and quantum information processing. Recently we have analyzed the exchange found in the transition-metal phthalocyanines;[11–14] since the magnetic moment is accommodated in the localized transition-metal *d* orbitals the exchange is relatively weak, though its strength depends on the *d*-orbital orientation.[12] In order to increase the exchange energy, an alternative is to use molecules where the unpaired electron is much more delocalized. One such candidate is lithium-phthalocyanine (LiPc, spin-$\frac{1}{2}$), shown in Fig. 1(a).

In the Hubbard-Anderson model (HAM) the strength of electron correlation can be measured by the ratio of on-site Coulomb interaction U to transfer integral t, i.e., $\frac{U}{t}$. The superexchange interaction emerges naturally at half-filling in the limit where U is much larger than t. Electron hopping lifts the degeneracy of spin states through second-order perturbation. The spin-excitation gap opened is proportional to the magnitude of superexchange interaction ($\frac{t^2}{U}$). When the ratio of U to t decreases below a critical value the ground state of the system described by the HAM can be a spin density wave (SDW) phase. In this phase spins are more itinerant, but still have localized characters (with reduced magnetic moment) inherited from localized magnetic state. SDW can therefore be understood as an intermediate phase between an antiferromagnetic insulator and a paramagnetic metal.

The HAM model may be applied to LiPc with the proviso that the U and t parameters refer to a molecular, rather than atomic, spin-carrying unit. Unlike Pc complexes formed with divalent metals, the monovalent Li can donate only a single electron to the Pc ring, giving rise to a singly occupied π orbital of the ligand. Such ligand orbitals are much more delocalized than transition-metal *d* states, and thus hybridize much more readily in the solid state; this implies that there is a larger t and a smaller U in LiPc than transition-metal-based materials. Hence a chain of LiPc molecules, with $\frac{U}{t} \sim 10$, represents a different class of systems to transition-metal phthalocyanines (TMPcs) such as copper phthalocyanine (CuPc) for which $\frac{U}{t} \sim 100$.[13] This relatively small $\frac{U}{t}$ value may also lead to a competition between localized and itinerant magnetic states such as SDW.

Measurements of the magnetic properties of LiPc have been performed in the known α, β, and *x*-LiPc phases in the temperature range 4 to 300 K.[15] These phases are distinguished by different chain geometries:[15] In the α and β phases the stacking angles (the angle between the line joining metal atoms and molecular plane) are small so the Pc rings are offset from one another along the chain axis, while in *x*-LiPc the rings are face-on, although twisted about the out-of-plane axis. Previous electron spin resonance (ESR) experiments[15] have suggested that α-LiPc has a ferromagnetic interaction of $\sim$4.5 K and β-LiPc an antiferromagnetic interaction between 3 and 37 K. The anisotropy of the ESR linewidths has been interpreted in terms of quasi-one-dimensional spin transport.[16] LiPc has also been used as a sensor material, with applications in magnetometry and oximetry,[17] and in the detection of oxygen and nitric oxide.[18]

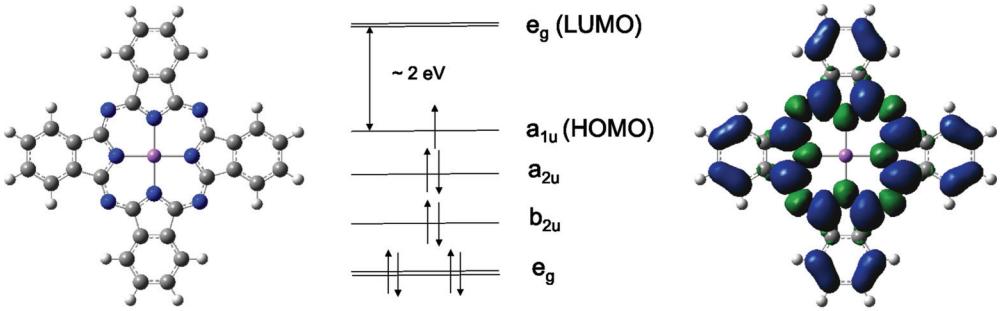

FIG. 1. (Color online) The single LiPc molecule: (a) molecular structure with Li in pink, C in gray, N in blue, and H in white; (b) sketch of the single-particle orbitals near the HOMO-LUMO gap; (c) spin density (spin-up density in blue and spin-down in green, with the isosurface value set to $0.001e/\text{Å}^3$). Notice that the spin density is spread into the whole molecule.

Previous theoretical studies have been restricted to computing the properties of monomers and dimers and using valence effective Hamiltonians to deal with the valence band and conduction band.[19–21] In consequence, an understanding of the relationship between molecular arrangement and magnetic properties is undeveloped. In this Rapid Communication we present first-principles calculations to establish the nature of magnetic properties and their variations with structure in LiPc chains.

Calculations have been performed for the stacking angles from 20° to 90° and sliding angles (determining the direction of neighboring molecular displacement) from 0° to 45° with 5° increments. Electronic correlation is important for the prediction of exchange coupling as the interaction scheme is complicated by the second- or higher-order many-body perturbation. The post-Hartree-Fock methods such as dedicated difference configuration interaction[22] can provide accurate results, but are computationally demanding. On the other hand, electronic correlation can also be taken into account using hybrid exchange density functional theory, which has previously been shown to provide a reasonable prediction of exchange interactions.[11–13,23] We have used density-functional theory (DFT) and the B3LYP hybrid exchange functional[24] to carry out calculations and alternative electronic exchange-correlation functionals to establish the robustness of our conclusions.[25] We find a crossover from a well localized antiferromagnet to a spin density wave ground state as the stacking angle increases, with an itinerant metallic state nearby in energy. The competition between these states may explain the complex magnetic behavior observed in the various LiPc phases.

Single molecule electronic structure. The computed energy level alignment of the Kohn-Sham orbitals near the HOMO (highest occupied molecular orbital)-LUMO (lowest unoccupied molecular orbital) gap for an isolated LiPc molecule are shown schematically in Fig. 1(b). The singly occupied HOMO, formed by the p_z orbitals of the ligand, has a symmetry a_{1u} (in D_{4h} symmetry). The Mulliken charge on the lithium is approximately $+0.3|e|$, confirming that the valence electron of lithium is significantly delocalized over the organic ligand. The computed HOMO-LUMO gap is ∼2 eV, which is consistent with that computed for TMPcs.[11–14] We have estimated the Hubbard-U for the a_{1u} orbital in the isolated LiPc molecule as the energy difference between the occupied spin-up and unoccupied spin-down orbitals, which is ∼4.6 eV. The delocalized nature of the HOMO is also apparent in the spin density, which is spread over the organic ring in accordance with a_{1u} symmetry as shown in Fig. 1(c). These theoretical results are in agreement with those from previous calculations[19–21] that have been used to explain the optical absorption and ESR measurements for LiPc.[16,17] The spin density of LiPc contrasts markedly with the localized spin densities computed in TMPc molecules.[3,11–14] The delocalization of the unpaired electron in LiPc suggests the nature of magnetic state and exchange interaction will be different in this material.

One-dimensional chain: Total energies and SDW instability. In order to analyze the change of the electronic properties of LiPc as the geometry varies, especially the competition between the nonmagnetic and magnetic states, we have calculated the total energies for a two-molecule supercell, in each structure in the range of stacking and sliding angles given above, in three states: ferromagnetic (FM), antiferromagnetic (AFM), and nonmagnetic metal (NM). For each sliding angle investigated here, $E_{\text{FM}} - E_{\text{NM}}$ changes sign from negative to positive at the stacking angle of 80°, and $E_{\text{AFM}} - E_{\text{NM}} < 0$.

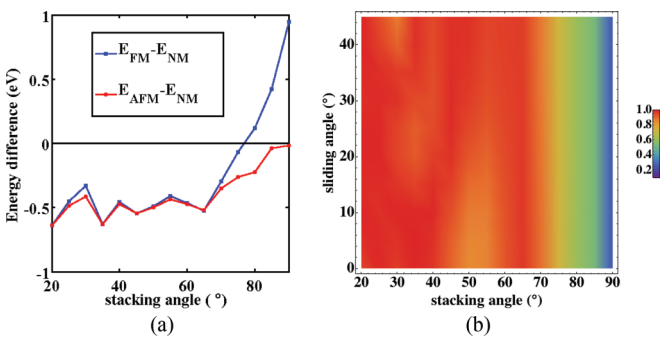

FIG. 2. (Color online) The differences between the total energies of the AFM (FM) and NM two-molecule supercells as a function of the stacking angle(the sliding angle is 45°) are shown in red (blue) in (a). The Mulliken spin densities per molecule in the AFM band structures are shown in (b). Notice that the NM state starts to drop below the FM state from the stacking angle 80°. In (b) the spin densities decrease away from the value of $1\mu_B$.

For small stacking angles, the AFM and FM states are close in energy and lie substantially below the NM state. As the stacking angle rises (towards the face-on configuration) the FM state rises in energy well above the NM state, which in turn approaches the energy of the AFM state. In what follows we refer to the geometry where the FM and NM states cross in energy (around a stacking angle of 80°) as *c*-LiPc. For larger stacking angles than this the AFM state is in competition with a metal; this suggests that the AFM state may itself become more itinerant in nature at such large stacking angles. This behavior is confirmed by the Mulliken spin density per AFM molecule shown in Fig. 2(b), which decreases monotonically with the stacking angle, being $\sim 0.6\mu_B$ for the *c*-LiPc geometry. This significant decrease of spin density from $1\mu_B$ (expected for localized spin) suggests a crossover from the localized AFM insulating state to an SDW.

We have also computed the energies of the FM, AFM, and NM states for the *x*-LiPc structure; here the energy of the NM state is higher than that of the AFM state by ∼22 meV per supercell. This value is comparable to the temperature (∼100 K) where the inverse susceptibility of *x*-LiPc starts to decrease as the temperature increases [see Fig. 5(a) in Ref. 15], marking a departure from the Curie-like local moment behavior seen at low temperatures. Furthermore, the computed spin density per molecule for *x*-LiPc is $\sim 0.2\mu_B$, which is also far below $1\mu_B$; this is consistent with the low effective moment seen in the Curie term.[15] Hence our calculations, and the available experimental evidence, suggest there is a phase transition between the SDW the and metallic state at ∼100 K.

One-dimensional chain: Band structures. Further insight into the states can be obtained from the single-particle band structures. The computed band structures for the FM configuration for α-LiPc, and the AFM configuration for β-LiPc, are shown in Figs. 3(a) and 3(b), respectively. The gap between the occupied and unoccupied a_{1u}-derived bands, which are almost flat, is ∼1 eV. This effective Hubbard-U in the LiPc chain is much smaller than that computed for copper-phthalocyanine[13] owing to the delocalized nature of the π state. It is also much

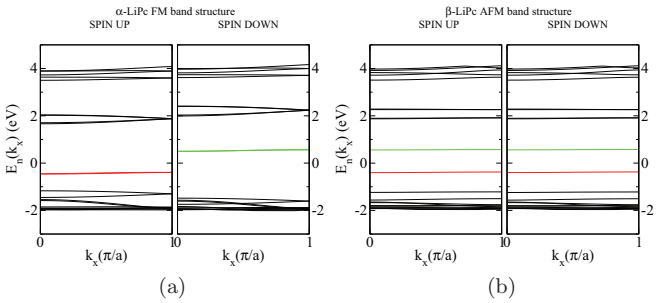

FIG. 3. (Color online) The FM band structures of α-LiPc (a) and the AFM band structure of β-LiPc (b) are shown, with the spin-up a_{1u}-derived bands in red and the corresponding spin-down ones in green. 21 bands are shown in each case. 12 (10) occupied for spin-up (spin-down) in the FM configuration for α-LiPc, and 11 occupied for each spin in β-LiPc. The Bloch wave vector k_x is oriented along the molecular stacking axis and the lattice constant a is for a two-molecule supercell. All energies are referred to the Fermi energy (for insulating states chosen to lie at midgap).

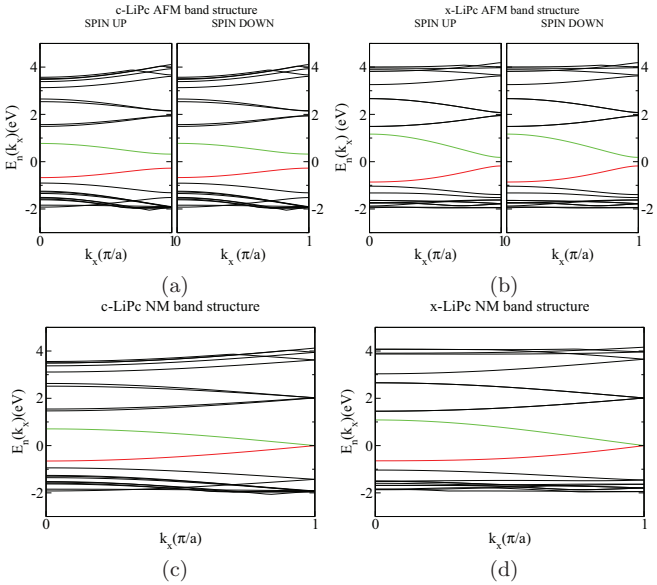

FIG. 4. (Color online) The AFM and NM band structures of *c*-(*x*-)LiPc are shown in (a) and (c) [(b) and (d)], respectively. 21 bands are shown, with 11 occupied in each case; the occupied a_{1u}-derived bands in red and the corresponding unoccupied ones in green. The Bloch wave vector k_x is oriented along the molecular stacking axis and the lattice constant a is for a two-molecule supercell. All energies are referred to the Fermi energy (for insulating states chosen to lie at midgap).

smaller than that computed in the isolated LiPc molecule; this indicates the effect of intermolecular interactions and screening. As shown in Fig. 4, *x*-LiPc and *c*-LiPc have a much larger dispersion of the single-particle states (corresponding to a larger effective hopping t) and the filled and empty a_{1u}-derived bands approach one another, being separated only by small gaps (∼0.5 eV for *c*-LiPc, ∼0.2 eV for *x*-LiPc).

These small gaps in the AFM band structures [see Figs. 4(a) and 4(b)] at the Fermi wave vector $k_F = \frac{\pi}{a}$ of the NM metal (a is twice the size of the chemical unit cell) are exactly as expected for a SDW commensurate with the Fermi-surface nesting in a half-filled band, i.e., $Q = 2\pi/a$. They provide further evidence for the existence of a SDW state when the stacking angle is equal to or larger than 80° and in *x*-LiPc. The crossover from localized *p*-orbital magnetism to SDW is driven mechanically by varying the stacking angle.

One-dimensional chain: Exchange interaction. The exchange interaction J is defined in a Heisenberg–Dirac–van Vleck-type Hamiltonian $\hat{H}^{\mathrm{HDVV}} = \sum_i 2J\hat{\vec{S}}_i \cdot \hat{\vec{S}}_{i+1}$, and is computed as $J = (E_{\mathrm{FM}} - E_{\mathrm{AFM}})/2$, where E_{FM} (E_{AFM}) is the total energy of a two-molecule unit cell with FM (AFM) spin configuration. We find $J/k_B \approx -39$ K (FM) and +4 K (AFM) for the α and β phases, respectively. These results are in qualitative agreement with previous magnetic measurements.[15] However, the magnitude of our theoretical result for the α phase is larger than that derived from the experiments $T_{CW} \sim 5$ K.[15] Our computed exchange for the β phase is in good agreement with the experimental results measured at the temperature below 50 K, but significantly smaller than that measured above 50 K.

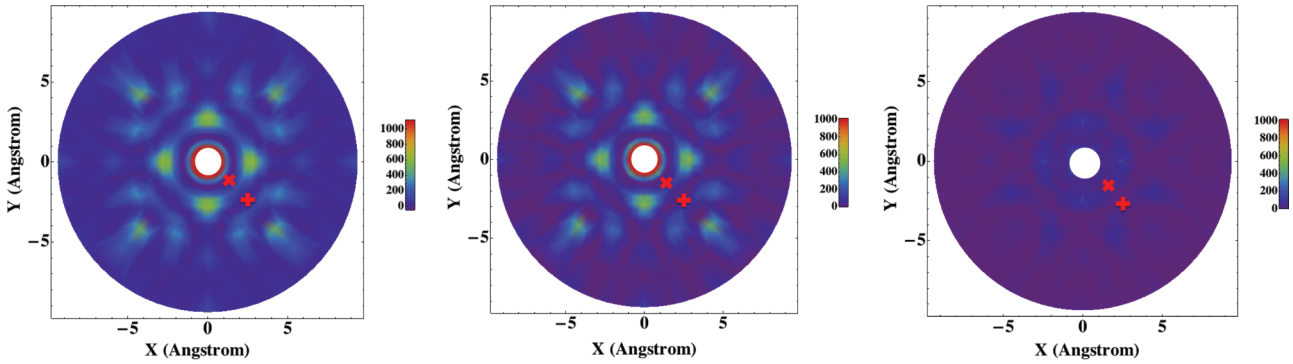

FIG. 5. (Color online) The exchange interaction J_{DFT} calculated using DFT total energies as a function of X and Y is plotted in (a), the corresponding superexchange estimate J_{SE} (see text) in (b), and their difference $|J_{\mathrm{DFT}} - J_{\mathrm{SE}}|$ in (c). Note the similar qualitative features in exchange interactions as a function of geometry. The cross ($\times$) and plus ($+$) signs label the geometries of the α- and β-LiPc phases, respectively.

Figure 5 shows the computed exchange interaction for the LiPc one-dimensional chain as a function of the components X and Y ($X = d \cot\phi \cos\psi, Y = d \cot\phi \sin\psi$), where d, ϕ, and ψ are interplane distance, stacking angle, and sliding angle,[25] up to the stacking angle 75°, after which point the SDW starts to develop. The exchange energy is seen to depend strongly on both stacking (corresponding to radial coordinate) and sliding angles (angular coordinate), in contrast to the situation in TMPcs where the dependence on the stacking angle is dominant.[12–14] Even at a small stacking angle ∼20° we can find a very large exchange interaction (∼275 K), owing to the highly delocalized nature of spin density in LiPc.

As the unpaired spin is highly delocalized, one might expect that an exchange interaction will arise from a combination of direct exchange and superexchange. In order to compare these contributions we have extracted the width (W) of the a_{1u}-derived bands and the Hubbard-U from the relevant FM band structures, and used them to estimate the superexchange interaction $J = \frac{2t^2}{U}$ (where $t = \frac{W}{4}$ is expected in a one-dimensional tight-binding model). As shown in Fig. 5, all the main features of exchange interactions calculated using DFT can be recovered by this simple superexchange model; we conclude that superexchange is the dominant interaction over most of the parameter space. The difference between the DFT exchange (J_{DFT}) and superexchange (J_{SE}) [Fig. 5(c)] couplings can be used to identify regions of parameter space where the direct exchange plays a relatively important role. The rapid variations of the exchange interaction can be understood from the spatial variation of the a_{1u} orbital. However, α-LiPc has a FM exchange interaction; we believe this is due to negligible transfer integrals between a_{1u} orbitals in this geometry [∼0.05 eV—see the flat bands in Fig. 3(a)] and a rather large direct exchange, leading to a pronounced FM interaction. The exchange interactions peak at a value of ∼1100 K at a stacking angle of 75°, which is much larger than those computed in the known phases of TMPcs[11–14] and typical organic magnets such as vanadium-tetracyanoethylene (V-TCNE).[26] This very large exchange interaction suggests that a room-temperature transition-metal-free antiferromagnet might be realized in LiPc if the molecular stacking can be controlled.

Discussions and conclusions. We have calculated the electronic structure of an isolated LiPc molecule and molecular chains using hybrid-exchange density functional theory. We have analyzed the total energies of different magnetic states, the spin densities per molecule, and the band structures. Our calculations show there exists a crossover from localized p-electron magnetism to a SDW at a stacking angle around 80°. Combined with available experimental results, our calculations also suggest that a transition occurs in the temperature regime from an SDW to a NM metallic state in x-LiPc at around 100 K.

Our calculated exchange interactions for the known α- and β-LiPc phases are in qualitative agreement with previous magnetic measurements;[15] our calculation for α-LiPc raises the possibility of a yet larger exchange interaction (∼39 K) and suggests that it might be possible to find high-temperature ferromagnetic spin-1/2 systems in phthalocyanine molecules. The exchange interactions have a complex dependence on *both* the stacking angle and the sliding angle; this dependence arises from the form of the HOMO. At the stacking angle of 20° we found a large antiferromagnetic exchange interaction ∼275 K, while the peak value of the computed exchange interactions is as high as ∼1100 K at a stacking angle of ∼75°, much higher than room temperature. The exchange mechanism is complicated by the delocalization of the singly occupied orbital; superexchange appears to be dominant over a large part of parameter space.

These results not only rationalize a poorly understood body of experimental data, but also reveal LiPc as a new type of material potentially possessing extremely high transition temperature, carrying p-orbital nanomagnetism, and showing intermediate electronic correlation and crossovers between localized and itinerant electronic behavior driven by simple structural parameters. We hope this work will inspire further work on this promising electronic and spintronic material.

Acknowledgments. We wish to acknowledge the support of the UK Research Councils Basic Technology Programme under Grant No. EP/F041349/1. We thank Gabriel Aeppli, Sandrine Heutz, Chris Kay, Giuseppe Mallia, and Marc Warner for helpful discussions.

*w.wu@imperial.ac.uk

[1]J. S. Miller, A. J. Epstein, and W. M. Reiff, Science **240**, 40 (1988).

[2]K. S. Kwok and J. C. Ellenbogen, Mater. Today **5**(2), 28 (2002).

[3]S. Heutz, C. Mitra, Wei Wu, A. J. Fisher, A. Kerridge, A. M. Stoneham, A. H. Harker, J. Gardener, H.-H. Tseng, T. S. Jones, C. Renner, and G. Aeppli, Adv. Mater. **19**, 3618 (2007).

[4]S. Pramanik, C.-G. Stefanita, S. Patibandla, S. Bandyopadhyay, K. Garre, N. Harth, and M. Cahay, Nat. Nanotechnol. **2**, 216 (2007).

[5]Z. H. Xiong, Di Wu, Z. Valy Vardeny, and Jing Shi, Nature (London) **427**, 821 (2004).

[6]V. N. Prigodin, N. P. Raju, K. I. Pokhodnya, J. S. Miller, and A. J. Epstein, Adv. Mater. **14**, 1230 (2002).

[7]S. Sanvito, Nat. Mater. **6**, 803 (2007).

[8]Jung-Woo Yoo, Chia-Yi Chen, H. W. Jang, C. W. Bark, V. N. Prigodin, C. B. Eom, and A. J. Epstein, Nat. Mater. **9**, 638 (2010).

[9]G. A. Timco, S. Carretta, F. Troiani, F. Tuna, R. J. Pritchard, C. A. Muryn, E. J. L. McInnes, A. Ghirri, A. Candini, P. Santini, G. Amoretti, M. Affronte, and R. E. P. Winpenny, Nat. Nanotechnol. **4**, 173 (2009).

[10]Hai Wang, S. Mauthoor, S. Din, J. A. Gardener, R. Chang, M. Warner, G. Aeppli, D. W. McComb, M. P. Ryan, Wei Wu, A. J. Fisher, M. Stoneham, and S. Heutz, ACS Nano **4**, 3921 (2010).

[11]Wei Wu, A. Kerridge, A. H. Harker, and A. J. Fisher, Phys. Rev. B **77**, 184403 (2008).

[12]Wei Wu, N. M. Harrison, and A. J. Fisher, Phys. Rev. B **88**, 024426 (2013).

[13]Wei Wu, A. J. Fisher, and N. M. Harrison, Phys. Rev. B **84**, 024427 (2011).

[14]Wei Wu, N. M. Harrison, and A. J. Fisher, Phys. Rev. B (to be published).

[15]M. Brinkmann, P. Turek, and J.-J. André, J. Mater. Chem. **8**, 675 (1998).

[16]H. Wachtel, J. C. Wittmann, B. Lotz, M. A. Petit, and J.-J. André, Thin Solid Films **250**, 219 (1994).

[17]J.-J. André and M. Brinkmann, Synth. Met. **90**, 211 (1997).

[18]R. P. Pandian, Young-Il Kim, P. M. Woodward, J. L. Zweier, P. T. Manoharan, and P. Kuppusamy, J. Mater. Chem. **16**, 3609 (2006).

[19]E. Ortí, J. L. Brédas, and C. Clarisse, J. Chem. Phys. **92**, 1228 (1990).

[20]M. Sumimoto, S. Sakaki, S. Matsuzakia, and H. Fujimoto, Dalton Trans. 31 (2003).

[21]M. Sumimoto, Y. Kawashima, D. Yokogawa, K. Hori, and H. Fujimoto, J. Comput. Chem. **32**, 3062 (2011).

[22]D. Muñoz, F. Illas, and I. de P. R. Moreira, Phys. Rev. Lett. **84**, 1579 (2000).

[23]F. Illas, I de P. R. Moreira, C. de Graaf, and V. Barone, Theor. Chem. Acc. **104**, 265 (2000).

[24]A. D. Becke, J. Chem. Phys. **98**, 5648 (1993).

[25]See Supplemental Material at http://link.aps.org/supplemental/10.1103/PhysRevB.88.180404 for more details about alternative functionals used and chain structure parameters.

[26]K. I. Pokhodnya, D. Pejakovic, A. J. Epstein, and J. S. Miller, Phys. Rev. B **63**, 174408 (2001).